Linking mass measured by the quartz crystal microbalance to the SI

C Stambaugh[1], H Shakeel[2], M Litorja[1] and J M Pomeroy[1]

[1] National Institute of Standards and Technology, Gaithersburg, MD 20899, United States of America
[2] Queens University Belfast, University Road, Belfast, BT7 1NN, Northern Ireland, United Kingdom

E-mail: corey.stambaugh@nist.gov and joshua.pomeroy@nist.gov

CrossMark

Abstract

Despite ubiquitous implementation of the quartz crystal microbalance (QCM) for measuring thin film thickness throughout industry and academia, a direct link to the SI (International System of Units) does not exist. Confidence in QCM measurements relies on over a half-a-century of academic and industrial research used to understand the resonant frequency change due to loading mass onto a quartz crystal. Here, we use before and after gravimetric mass measurements, linked directly to the SI, to measure mass change. A custom vacuum metal deposition system is used to deposit gold films of various masses onto a series of quartz crystals while the mass dependent frequency change is monitored in real time. The gravimetric (known) mass changes are compared to three analytical methods (frequency, time and energy) used to convert resonant frequency shifts to mass changes, none of which rely on the material properties of the deposited material. Additionally, we evaluate the reversible and irreversible contributions to mass change from the loading into, and removal from, the vacuum environment. We find the energy-based method for frequency to mass conversion has the best accuracy over the longest range, at 0.36 % to >1 mg. Only for mass changes below 100 µg are deviations >2 % observed. A complete uncertainty budget is provided.

(Some figures may appear in colour only in the online journal)

1. Introduction

The quartz crystal microbalance, or QCM, is a resonance-based sensor that is commercially available at low cost, making it highly attractive for a wide range of uses; the most common being thin film deposition monitoring. The crystal frequency change can be calibrated to a specific system using a variety of materials and geometric factors that provide robust, *in situ* measurements of thin film thickness. Beyond this prototypical use, functionalized QCMs are also used for a variety of biomedical applications including immunosensors [1]. Furthermore, the QCM is easily integrated into micro-electronics making it viable for embedded applications [2, 3] and it has been deployed as a research tool for liquid-based applications [4]. The use of the QCM for thin film monitoring also makes it an intriguing tool for studying sorption effects on mass artifacts [5].

A long-standing challenge in precision mass metrology is the variation of an artifact's mass over time. This process, driven by both physical and chemical sorption effects, can be even more pronounced when mass artifacts are transported to customers or other metrology institutes because of the varying environmental conditions, i.e. temperature, pressure, and humidity. For example, air quality varies across the globe, leading to higher levels of contaminants and the potential for physi- and chemisorption-based processes to occur. This can result in unpredictable shifts in the calibrated value of the mass artifact. A possible solution to this is the use of a well characterized resonance-based sensor that can travel with masses to provide an indication of possible mass change [6, 7].

An extreme example of such an environmental change is moving from vacuum to air. The adsorption of hydrocarbons and water molecules is known to change the mass of 1 kg artifacts by tens of micrograms [8]. This is of particular relevance in light of the recent redefinition of the kilogram [9] because instruments like the Kibble balance will determine the absolute mass of an artifact in vacuum while the dissemination must still take place in air [10]. Therefore, detailed knowledge of the mass shift from the adsorption process is required. Currently, to quantify the mass change, artifacts having similar characteristics, but dramatically different surface area are used to measure the differential desorption rate in air and vacuum [8]. Resonator based sensors, like the QCM, could provide additional insight into the surface sorption effects that occur by providing real-time monitoring of the mass change [11], but these measurements are not yet connected to the SI unit of mass [6]. We provide a preliminary example of monitoring the vacuum-air mass change below as a part of this work.

In this paper, we assess the accuracy and precision of frequency-based measurement techniques for quantifying the mass of a thin film deposited onto a QCM by directly comparing to an SI-traceable, gravimetric-based, mass measurement approach. Three methods are compared for calculating the mass from the frequency change: (1) the traditional frequency-based or Sauerbrey equation method [12], (2) the so-called period or time method [13], and (3) the energy method [14]. All three methods are independent of the deposited films material properties, allowing an examination of the QCM's general ability to determine mass changes, irrespective of the material. While some previous works have similarly examined these dependencies [13, 15–17], here we establish direct traceability to the SI unit of mass, the kilogram. Additionally, most prior works have focused on the areal density (mass per unit area), ignoring the challenge of accurately measuring the area of deposition in order to find an absolute mass. As we will show, the areal uncertainty is the leading source of error in determining absolute mass.

Here, the QCM's gravimetric mass is measured using a double-substitution technique with OIML E1-class mass standards calibrated at NIST using an electrostatic force balance [18]. The mass of the QCM was measured before and after the deposition of gold films of varying thicknesses. This experiment allows us to (a) validate the use of the QCM for accurate small mass measurements and (b) study the QCM's efficacy for quantifying the sorption process, enabling focused studies on both vacuum to air transfer and long-term mass tracking of artifacts.

2. Theory

Since QCMs are already widely in use, we chose to utilize the cheap, consumable crystals available from many sources in the market. Figures 1(A) and (B) show example photographs of the commercial QCMs used in our experiment before (as provided by manufacturer) and after the deposition of additional gold. The addition of mass onto a QCM leads to an effectively
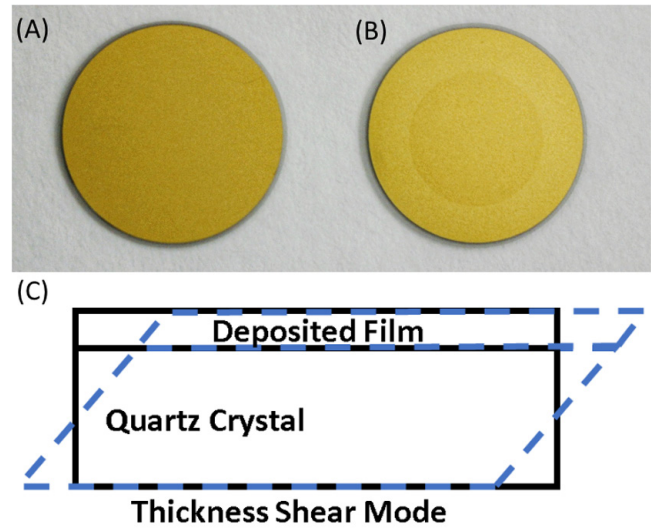

Figure 1. Photograph of two $\approx 1\,\mathrm{cm}^2$ QCM crystals (A) before loading and (B) after loading. The deposited film is the faint circular spot on the gold electrode in (B) corresponding to run 34 in table 1. (C) The QCM resonates in the thickness shear mode with a resonance $f_q = v_q/(2t_q)$, where v_q is the shear wave velocity along the thickness direction and t_q is the thickness. In general, the deposited film can be viewed as increasing $t_q = t_q + t_d$, where t_d is the thickness of the deposited film.

thicker crystal, which lowers its resonant frequency; see caption of figure 1. The resonant mode of interest, as noted in figure 1(C), is the thickness shear mode. The link between this change in resonant frequency (Δf) and the change in mass (M_f) resulting from the addition of the thin film onto the QCM surface was first described by Sauerbrey, in what is commonly known as the Sauerbrey equation [12]:

$$M_f^S = - \left(\frac{N_q \rho_q A}{f_q} \right) \frac{\Delta f}{f_q}. \tag{1}$$

Here, $\Delta f = (f_q - f_c)$, where f_q is the original frequency of the quartz crystal, and f_c is the frequency of the coated crystal. The area of the deposition is noted as A, while the constant ρ_q and N_q refer to the density and crystal constant of the quartz crystal; values for AT-cut crystals are $\rho_q = 2.648\ \mathrm{g \cdot cm^{-3}}$ [19] and $N_q = 1.668 \times 10^5\ \mathrm{Hz \cdot cm}$ [20] (uncertainties in table 3). The prefactor $(N_q \rho_q A)/f_q$, which assumes a uniform, cylindrically-shaped, deposition volume is the mass of the active area of the quartz crystal, M_q. Dividing the term by f_q provides a useful estimate of the resonator's mass sensitivity, $S_T = M_q/f_q$ [15]. In this case, equation (1) becomes $M_f^S = -S_T \Delta f$. In the experimental section below, this is the first method used to calculate mass from the change in frequency.

While equation (1) has been shown to be a reasonable approximation for frequency to mass conversion, it has its drawbacks. Primarily, it assumes that the deposited film is identical to quartz and the frequency shift caused by the additional mass does not impact the sensitivity of the crystal during deposition. This leads to measurable deviations of the calculated mass from the actual mass change for frequency shifts $>0.5\,\%$ or $\approx 200\ \mu\mathrm{g}$.
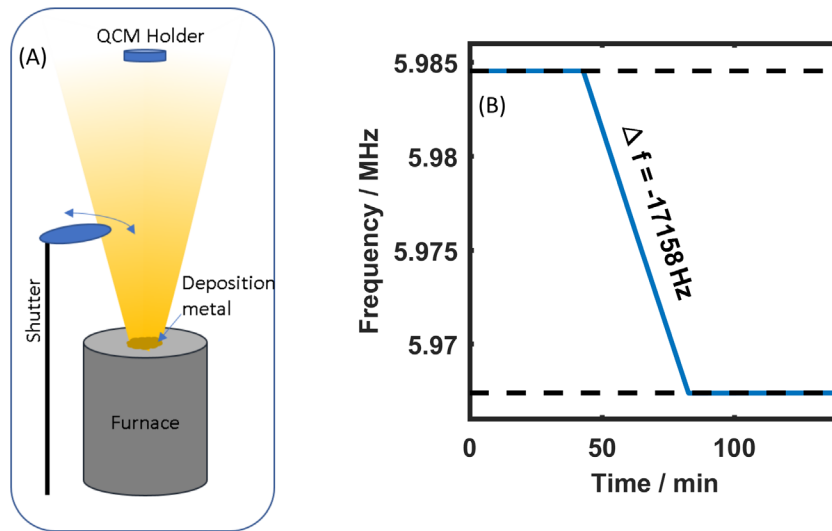
Figure 2. (A) Simplified schematic of the basic experimental apparatus. The QCM is placed at the top of a vacuum chamber with the top side (figure 1(A)) directed toward a furnace with molten gold whose fluence can be started and stopped with a shutter. (B) As gold is added onto the QCM surface, the resonant frequency decreases proportionally (run 5).

A second, period-based method, addresses these concerns by dividing the frequency shift by the frequency of the coated crystal:

$$M_f^T = -S_T \Delta f \frac{f_q}{f_c}. \tag{2}$$

This method better approximates the change in mass but lacks an analytical basis for the change from f_q to f_c [14]. This is also the second method calculated in the experimental section below.

The third method is known as the energy method [14], and is derived by considering the energy loss that occurs from the added film. Assuming the deposited film covers the entire active area of the crystal, the mass-frequency relation can be written as:

$$M_f^E = -S_T \frac{f_q}{2} \left(\frac{1}{(1-\Delta f/f_q)^2} - 1 \right)$$
$$= -S_T \Delta f \left(\sum_{i=0}^{\infty} \left(\frac{\Delta f}{f_q} \right)^i (i/2 + 1) \right). \tag{3}$$

Here, the $i=0$ terms returns equation (1) and the first order term $i=1$ provides a very good approximation ($<0.2\%$) of the unexpanded form of equation (3) for small ($<3\%$) frequency changes.

The typical starting frequency for the QCMs used here was approximately 6 MHz. Inserting this frequency, along with the other constant terms, gives a mass sensitivity of $S_T \approx 6.7 \, \mathrm{ng \cdot Hz^{-1}}$. In a nitrogen environment, at a stable temperature, the frequency is stable to ≈ 0.2 Hz, and a mass sensitivity of $\approx 1.3 \, \mathrm{ng}$. Finally, since most works on QCMs refer to areal density, we state the areal sensitivity $s_T = 12.32 \, \mathrm{ng \cdot Hz^{-1} \cdot cm^{-2}}$.

3. Experimental method

Our experimental strategy is to compare the mass derived from the QCM resonant frequency due to the deposition of gold with the change in the SI traceable gravimetric mass. The following procedure was followed for the measurement of each QCM:

  (i) Initial gravimetric mass comparison;
 (ii) Initial frequency measurement;
(iii) Evacuation of chamber, deposition of material, and purging of chamber;
(iv) Final frequency measurement;
 (v) Final gravimetric mass comparison.

This procedure was used to measure the mass and frequency change of all tested QCMs. The change in frequency over the course of the deposition, figure 2(B), is then converted to a change in mass from the deposited film using the three methods in equations (1)–(3) and compared with the (known) gravimetric mass change.

3.1. Gravimetric mass method details

The gravimetric-based mass comparisons are performed using a mass comparator with 0.1 μg resolution and a set of masses that are NIST traceable to the SI. The traceability to the SI is made using the electrostatic force balance (EFB), which relies on the newly fixed value of Plancks constant [21] to connect a voltage measurement to the unit of mass [18]. This is just one example of the new possibilities enabled by revising the SI to be based on a set of fundamental constants [22]. This approach provides the lowest possible uncertainty for gravimetric measurements at the milligram level [18].

The true mass of the QCM is calculated as:

$$M_{\mathrm{qcm}} = M_{\mathrm{ref}} + \Delta M_{\mathrm{qcm,ref}} + \rho_{\mathrm{air}} \cdot (V_{\mathrm{qcm}} - V_{\mathrm{ref}}). \tag{4}$$

Here M_{ref} is the calibrated mass of the working standards that were calibrated using the primary weights from the EFB. The term

$$\Delta M_{\mathrm{qcm,ref}} = \frac{(M_{\mathrm{qcm}}^1 + M_{\mathrm{qcm}}^2)}{2} - \frac{(M_{\mathrm{ref}}^1 + M_{\mathrm{ref}}^2)}{2} \tag{5}$$

is the measured mass difference of the QCM and working standard using the double substitution or ABBA method of mass comparisons, where subscripts QCM and REF denote the A and B components of the measurement, and the superscripts indicate their respective measurement order. The terms with superscript 1 or 2 represent the mass values as recorded from the mass comparator and have not been corrected for effects such as buoyancy. The final term is the air buoyancy term where the air density ρ_{air} is calculated from Picard [23], while the volumes V_{ref} are determined from the density and known mass of each weight. For the purpose of calculating the buoyancy effect, we use an effective density $\rho_{qcm} = 2.648 \text{ g} \cdot \text{cm}^{-3}$ for the quartz crystal. The gold electrodes may cause the actual density to deviate from this value by $\approx 1\%$, but this will not affect the final result since the change in buoyant term is less $<0.3\,\mu\text{g}$ (see table 2). The working standards are made of stainless steel and have a density $\rho_{ss} = 8.03 \text{ g} \cdot \text{cm}^{-3}$. Since the mass of the QCM is initially unknown, the measured gravimetric value is used to estimate the volume V_{qcm} using the density so the buoyancy can be taken into account. The resultant mass is then used to reestimate the volume as the true mass is recalculated.

The mass change of the QCM from before (i) and after (f) the deposition of gold is the quantity of interest and given by:

$$M_g = M_{qcm}^f - M_{qcm}^i$$
$$= \left(M_{ref} + \Delta M_{qcm,ref}^f + \rho_{air}^f \cdot (V_{qcm}^f - V_{ref}) \right)$$
$$- \left(M_{ref} + \Delta M_{qcm,ref}^i + \rho_{air}^i \cdot (V_{qcm}^i - V_{ref}) \right). \quad (6)$$

Upon simplifying, several terms drop out. These terms, while not in the final equation, served a crucial role of anchoring the mass measurements before and after deposition to the SI unit of mass, the kilogram. This ensures that the balance is properly calibrated, and its reading has not changed over time. The gravimetric mass of the deposited film can now be expressed as:

$$M_g = \Delta M_{qcm,ref}^f - \Delta M_{qcm,ref}^i + \rho_{air}^f V_{Au}$$
$$+ (V_{qcm^i} - V_{ref}) \cdot (\rho_{air}^f - \rho_{air}^i) \quad (7)$$

where the volume of the deposited gold film is $V_{Au} = V_{qcm}^f - V_{qcm}^i$. The gravimetric-based result of the mass change, M_g, is the accepted value for the mass of the deposited gold. It will be compared to the mass value, $M_f^\times$ (where $\times = S$, T, or E, see section 2), derived from the measured frequency shift resulting from the deposition of gold as described in the next section.

3.2. Frequency method details

The experimental setup for the deposition and frequency measurement is shown in figure 2(A). The QCM is mounted, facing downward, in a vacuum chamber. Less than 10 cm below the QCM is a pneumatic shutter used to control when the deposition starts and stops. Positioned approximately a half-meter below the QCM is the gold furnace. The QCM is aligned to within 1 cm of the principal axis of the furnace.

Based on these measurements, we expect the distribution of flux across the QCM to deviate by less than 0.1% [24]. Additionally, since the QCM is the substrate of interest, our tooling factor is 100%. The tooling factor, typically used for thickness monitoring applications, is a correction factor that accounts for the position dependence of the deposition rate. This is often needed because the substrate of interest and the quartz crystal, normally, cannot be co-located. A frequency counter is used to monitor the frequency of the QCM before, during and after the deposition process.

Once the QCM is loaded in the vacuum chamber, nitrogen is flowed in to the chamber until a pressure of ≈ 1.3 kPa is reached. The QCM is left in this condition for approximately two hours while its frequency, the chamber pressure and temperature near the QCM is monitored. During this time, the final gravimetric measurements of the previous QCM, post deposition, are made. After the initial frequency measurement, the chamber is pumped down for 30 h, so that pressure is $\approx 1 \times 10^{-6}$ Pa. Starting with the pump down, the need for operator control is kept to a minimum through automation thus minimizing random process deviations.

Once pumped down, the furnace turns on and the temperature is slowly raised to 1000 °C. This temperature is held for several minutes, then raised through PID control and setpoint tracking to ≈ 1480 °C where it sits for another 5 min. After the short delay, the shutter automatically opens, and deposition of gold commences. During the whole procedure, the QCM frequency, vacuum pressure and temperature at the furnace and near the QCM are monitored. The shutter is left open until the desired frequency shift occurs. Once the shutter closes, the furnace is slowly cooled down to room temperature over the course of several hours. In this paper, two sets of data are presented. For the first, set A, the process described above was performed manually, while for set B the process was automated, and each set was measured by a different operator.

After cooling down for ≈ 8 h, the chamber is purged with nitrogen, bringing the chamber pressure back up to the initial 1.30 kPa. The QCM is left in this condition and frequency data is acquired for another 60 min. During this time the gravimetric mass of the next QCM to go into the chamber is measured. By making gravimetric measurements in this way, the time outside of the chamber either before (for initial) gravimetric mass measurements are made or after (for final) is kept to a minimum. The total time between initial and final gravimetric measurements for *set B* was held to about 2 d, while for *set A* the time varied from days to as long as weeks.

3.3. Area of deposition

While the initial frequency is known, and the values of the crystal's density and crystal constant of the quartz crystal can be found in the literature, accurately identifying the area of deposition is challenging. This is one reason most QCM mass readings are given in areal mass (mass per unit area). Here we outline two approaches for measuring the deposition area. First, the aperture size of the QCM holder was measured using an SI-traceable coordinate measuring machine with

Table 1. Values for measured frequency shifts and mass changes for deposition of gold on to QCM's. Set B has been re-ordered in terms of total mass deposited, the run number reflects the actual measurement order. Here, $\Delta M = M_f^E - M_g$.

Set	#	Δf (Hz)	M_g (μg)	u_{M_g} (μg)	M_f^E (μg)	$u_{M_f^E}$ (μg)	ΔM (μg)
A	1	7492.8	52.30	0.57	50.39	0.14	−1.91
	2	7553.5	52.50	0.64	50.79	0.15	−1.71
	3	17 159.2	116.90	0.57	115.79	0.33	−1.11
	4	17 166.0	117.00	0.64	115.54	0.33	−1.46
	5	17 158.6	117.80	0.57	115.72	0.33	−2.08
	6	17 159.5	116.90	0.64	115.59	0.33	−1.31
	7	32 253.0	220.20	0.64	218.00	0.62	−2.20
	8	47 217.1	320.40	0.72	320.73	0.91	0.33
	9	62 536.0	427.60	0.64	426.19	1.21	−1.41
	10	77 498.9	529.30	0.57	530.15	1.51	0.85
B	30	2473.5	16.87	0.34	16.64	0.05	−0.23
	25	7793.8	53.19	0.85	52.39	0.15	−0.80
	29	12 780.8	87.77	0.35	86.11	0.25	−1.66
	24	18 111.6	122.48	0.47	121.45	0.35	−0.48
	22	23 609.8	160.30	0.45	159.29	0.45	−1.01
	26	24 265.0	164.81	0.62	164.0	0.47	−0.81
	27	40 590.0	280.62	0.13	275.37	0.78	−5.25
	28	53 988.6	363.93	0.18	367.33	1.04	3.40
	23	64 093.3	440.81	0.66	438.11	1.25	−2.70
	34	105 152.0	722.63	0.13	726.12	2.07	3.49
	33	150 059.3	1044.26	0.12	1047.24	2.98	2.98

an interferometer for encoding optically-detected edge point positions around the aperture perimeter [25]. The coordinates are then fit to a circle to determine the area. The measured area was $(0.5445 \pm 0.000\,25)$ cm^2.

Second, we took optical images of the deposited area of gold on the QCM surface. Imaging such a large area, with small features, requires utilizing the stitching capability of modern imaging software. A set of 9 images are taken and overlaid to produce the final image. The translation of the image between acquisitions is done using an X-Y stage with an optical encoder. This provides a reference for the overall size of the image. Once the image is acquired, an edge detection algorithm is used to extract a set of points from around the image edge. The set of points can be fit to an ellipse to determine the overall area. The measured area, based on this method, for QCM (run 7) was (0.544 ± 0.003) cm^2.

The two stated methods for determining the deposition area agree to within their uncertainties. In our analysis, we used the value 0.5445 cm^2, which came from the aperture measurements. This value is chosen, since it can be measured before the measurement and applied to the analysis of all QCM deposited using the same holder.

4. Uncertainty analysis

The aim of this work is to fully characterize the mass measurement capability of the QCM. A complete uncertainty analysis therefore is essential. The measurement can be broken down into two components: frequency-based and gravimetry-based. We will tackle the uncertainty associated with each separately.

4.1. Gravimetric method uncertainty

The uncertainty of the gravimetric mass measurement results from 3 main components. The first is the uncertainty of the working standard. The second results from the comparison of the QCM with the working standard–this includes the resolution of the mass comparator. The third is due to the buoyancy correction, which encompasses the uncertainty from the density of the materials, as well the environmental factors (pressure, humidity, and temperature). Since a double substitution (ABBA) comparison is being performed, the uncertainty of the working standard is common to the QCM measurements before and after deposition and thus drops out.

The buoyancy term for gold is $M_{Au}^B = \rho_{air} \times V_{Au}$. Because the volume of deposited gold is small, the buoyant force contributes less than 0.1 μg to the total mass. The buoyant force contributed by the reference standard and the QCM is $\Delta M_{qcm,ref}^B = (V_{qcm}^i - V_{ref}) \times (\rho_{air}^f - \rho_{air}^i)$. During the 48 h period between measurements, the air density does not change by more than 1 %. The largest resulting buoyant correction is just under 0.3 μg, though typically much less. The uncertainty on both terms is below the balance resolution of 0.1 μg so for the gravimetric measurements, only the terms $\Delta M_{qcm,ref}^{i,f}$ from equation (7) contribute to the final uncertainty. These terms are noted $u_{\Delta M_{qcm,ref}^{i,f}}$ and their values are based on the standard deviation of five complete ABBA measurements. The total uncertainty in the mass of the deposited gold film is therefore:

$$u_{M_g} = \sqrt{(u_{\Delta M_{qcm,ref}^i})^2 + (u_{\Delta M_{qcm,ref}^f})^2}. \qquad (8)$$

Table 2 contains values for each term in equation (7).

Table 2. Uncertainty budget for the gravimetric measurement of the deposited gold film. The upper table provides the values needed to account for buoyancy. The lower table contains the values and uncertainty contributions from equation (7). While the initial mass of the QCM varied between samples, the absolute difference between it and the reference mass, both before and after deposition, was always less than 1.5 mg.

	Value	u_x	$u_x/|x|$
Buoyancy			
ρ_{air} (mg · cm^{-3})	($\sim$1.181)	4.0×10^{-4}	$<3.3 \times 10^{-4}$
V_{ref} (cm^3)	0.0112	1×10^{-5}	3×10^{-4}
V_{qcm} (cm^3)	0.0340	1×10^{-5}	$<1 \times 10^{-4}$
V_{AU} (cm^3)	$<5.2 \times 10^{-5}$	1×10^{-8}	$<2 \times 10^{-3}$
Mass			
$|\Delta M_{\text{qcm,ref}}^{i,f}|$ (μg)	<1500	<0.8	
$\Delta M_{\text{qcm,ref}}^{B}$ (μg)	<0.3	$<3 \times 10^{-2}$	
M_{Au}^{B} (μg)	<0.1	$<5 \times 10^{-5}$	
M_g total (μg)	17–1044	<0.8	0.0001–0.018

Table 3. Uncertainty budget for the frequency to mass determination, which is dominated by the area uncertainty. For total uncertainty, the largest relative error is given.

|	Value	u_x	$u_x/|x|$
N_q (Hz · cm)	1.668×10^5	0.001×10^5	5.9×10^{-4}
ρ_q (g · cm^{-3})	2.648	0.001	3.8×10^{-4}
A (cm^2)	0.5445	0.0015	$<2.8 \times 10^{-3}$
f_q (Hz)	6×10^6	1	1.7×10^{-7}
Δf (Hz)	(1000–15 000)	1	$<1 \times 10^{-3}$
$M_f^{\times}$ total			$<3.0 \times 10^{-3}$

4.2. Frequency method uncertainty

The uncertainty of the frequency-based method has two parts: (a) that rooted in the sensitivity term S_T, which is composed of the QCM material properties, the area of deposition, and initial frequency; and (b) those related to the frequency component where only the first order term Δf is significant. The overall fractional uncertainty is then:

$$\frac{u_{M_f^{\times}}}{M_f^{\times}} = \sqrt{\left(\frac{u_{S_T}}{S_T}\right)^2 + \left(\frac{u_{\Delta f}}{\Delta f}\right)^2}. \quad (9)$$

The contribution from (a) is:

$$\frac{u_{S_T}}{S_T} = \sqrt{\left(\frac{u_{N_q}}{N_q}\right)^2 + \left(\frac{u_{\rho_q}}{\rho_q}\right)^2 + \left(\frac{u_A}{A}\right)^2 + \left(2\frac{u_{f_q}}{f_q}\right)^2} \quad (10)$$

where terms u_{N_q}, u_{ρ_q}, u_A and u_{f_q} are the respective uncertainties for the crystal constant, quartz density, area of deposition and the quartz crystal frequency. Table 3 lists the overall value for each term, the uncertainty and the fractional uncertainty. For the frequency component, the largest fractional uncertainty (i.e. smallest frequency shift) is given.
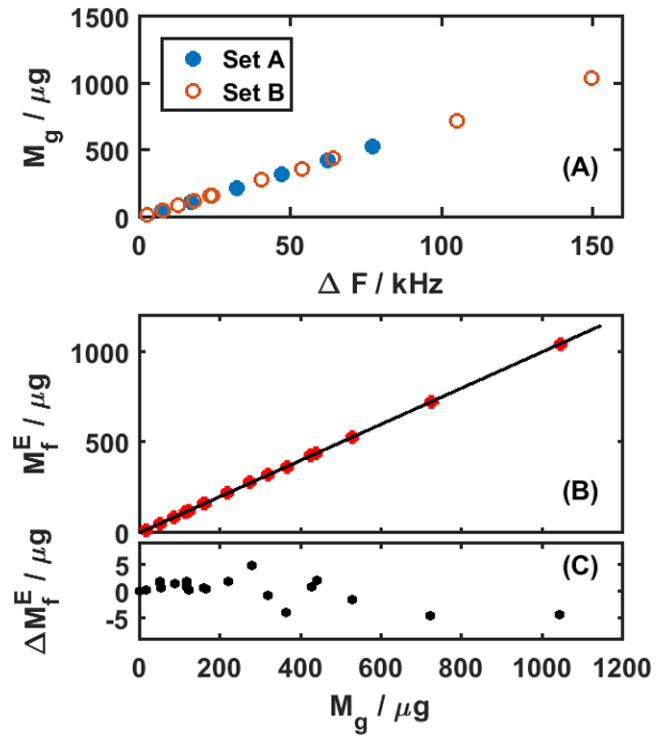

Figure 3. (A) Plot of measured gravimetric mass change versus frequency shift resulting from the deposition of gold. The two data sets were taken by different operators and over a year apart. Between runs the deposition system underwent numerous changes, including the introduction of cooling water for the QCM and furnace, as well as the introduction of an automated deposition process. Despite the various differences, the results are in excellent agreement with each other. (B) Calculated mass (M_f^E) derived from the frequency shift using equation (3) versus the measured gravimetric mass (M_g) of the film. The data is fit to a line through with 0 offset and the slope is $(0.9987 \pm 0.0036)\ \mu\text{g} \cdot \mu\text{g}^{-1}$. (C) A plot of the fit residuals ΔM_f^E. Note—the uncertainties (shown in table 1) are too small to see in (B) and (C).

5. Results and discussion

Table 1 has a complete list of the measured frequency shifts and the corresponding gravimetric change in mass, which are graphically represented in figure 3(A). The two sets of data, *set A* and *set B* were taken about one year apart, by two different operators and the gravimetric masses in *set A* were measured by a third person. Finally, as mentioned earlier, the deposition process was upgraded to be completely automated before *set B* was taken. Therefore, the two data sets are substantially independent, yet as shown by figure 3(A) the results from the two data sets are in excellent agreement. The remainder of the analysis will treat the two sets as one complete set.

The two outstanding questions we seek to answer are: (1) which method of frequency to mass conversion provides the best result, M_f^S, M_f^T or M_f^E and (2) how well does the QCM predict the actual change in mass? The second question is addressed in figure 3(B), which shows plots of the calculated mass from the frequency shift using the energy-based
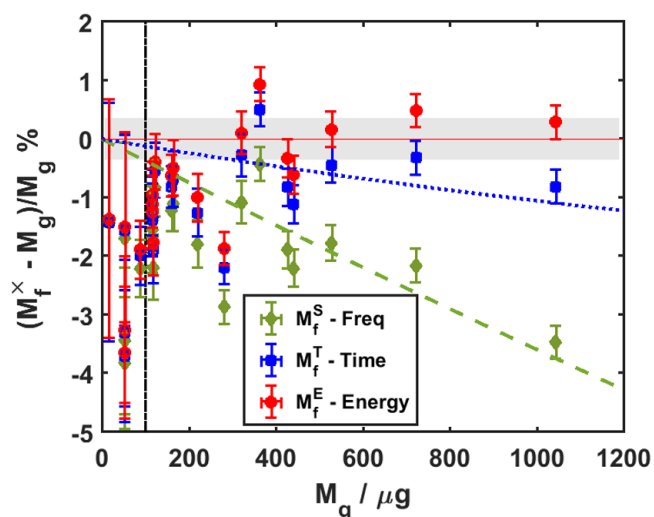
Figure 4. The percent error between the QCM measured mass and the gravimetric measured mass for each of the three analytical methods used to convert resonant frequency shift to mass change is shown. The increasing deviation when using the 'standard' frequency approach (M_f^S, equation (1)) is clear. The width of the gray bar represents the standard deviation for the fit in figure 3(B). The solid, dotted and dashed lines correspond to the expected deviation, based on equations (3), (2), and (1), of the frequency-based mass measurement for increasing mass values.

method (equation (3)) versus the gravimetric mass. The data are fit to a line whose intercept is forced to be zero. The fit is weighted according to the relative errors of the data and the residuals are shown in figure 3(C). In the ideal case the slope is exactly one, while the slope in figure 3(B) is (0.9987 ± 0.0036) μg · μg^{-1}. While not plotted, the corresponding slopes when converting frequency to mass using equations (1) and (2) give (0.978 ± 0.0044) μg · μg^{-1} and (0.9925 ± 0.0030) μg · μg^{-1}, respectively. The energy-based method shown gives the most accurate result. The standard method of Sauerbrey is the furthest off. Since the Sauerbrey method does not account for the effects of the film on the QCM response (i.e. the change in the absolute frequency of the quartz crystal), it is expected to underestimate the mass change as the film grows thicker. While figure 3(B) shows that an accurate conversion from frequency to mass can be made using the energy method, this approach does obfuscate how far each data point deviates from its expected value.

In figure 4, the data is plotted as the percent error relative to the accepted value (gravimetric-based). Again, it is clear the energy-based method provides the overall best result for the complete range. However, now a few other details are revealed. First, for small mass changes (<100 μg), or frequency shifts (<0.25%), all the methods underestimate the mass change by more than 1%. Second, as the thickness increases, the Sauerbrey method increasingly underestimates the mass change, while both the period and energy-based approaches have decreasing relative errors. This is attributed to those two methods accounting for the increasing thickness. Finally, over the majority of the range, the energy method was able to accurately convert frequency change to mass to within 1% the accepted values.

As the large error bars suggest, the accurate measurement of small masses is difficult. The smallest mass shift was (16.87 ± 0.34) μg, and its associated frequency-based mass shift was 16.64 μg, a difference of 0.23 μg. The balance itself had a readability of 0.1 μg, so a small systematic uncertainty could explain the deviation for the smaller mass shifts, since this would have diminishing effect with increasing mass. None-the-less, the results still show that mass changes below <100 μg can still be reliably measured using the QCM with errors of only a couple of percent.

As pointed out previously, the introduction of an artifact into a vacuum environment can lead to a change in mass. Discussed further elsewhere [8, 10], the process is expected to be largely reversible. Throughout the measurements we observed a change in frequency moving from air to nitrogen to vacuum of $(12 \pm 2$ Hz), and $(7 \pm 2$ Hz) when going back to nitrogen. We performed one test where no mass was deposited and instead we purged and pumped several times. The results showed the change in frequency for pumping process tend towards the 7 Hz, while the purging process stayed at 7 Hz. Overall, this agrees with the expected behavior of moving between vacuum and air. When converted to mass, we find that this represents a reversible mass change of approximately 47 ng (86 ng · cm^{-2}), and a possible irreversible desorption when moving into (oil-free) vacuum of 34 ng (62 ng · cm^{-2}). This measured reversible change between vacuum and nitrogen agrees with previous QCM measurements [11].

6. Conclusion

We have examined the accuracy of mass measurement using the QCM by comparing results from three methods with comparisons to SI traceable masses. Two sets of data were acquired by two different operators approximately one year apart. The operators worked independently of each other and the second set of data was carried out using an automated deposition system. The agreement of the two data sets demonstrate the reliability of the measurements.

Overall, the results demonstrate that the energy-based method given in equation (3) is the most accurate over the largest range, while still not depending on the exact film properties. Furthermore, our results show that the area of mass deposition can be determined either before by accurately measuring the aperture or after by imaging the deposited area. While the value of the area introduces the largest component of uncertainty, results with uncertainty below 1% are clearly achievable. When the proper model is applied, and the aperture is well characterized, the QCM can accurately measure absolute mass change. For very small mass changes (<100 μg) the uncertainty exceeds 1%, but the QCM accuracy still stays within 4%. These results are strictly applicable to stiff films; for more viscous materials larger deviations are expected.

Finally, all the gravimetric measurements made are directly traceable to the SI unit of mass. Thus we have shown that frequency-based measurements of mass using a QCM can be tied directly to the SI unit of mass. This demonstrates that SI traceable, real-time mass monitoring is possible.

Such an approach could be useful for monitoring how mass changes in environments that vary over time. Furthermore, the redefined SI opens new approaches for the measurement of mass, results like the ones shown here are critical to bridging the gap between conventional mass metrology and the new opportunities that micro- and nano-based sensors afford within the new SI.

ORCID iDs

C Stambaugh ⬤ https://orcid.org/0000-0001-9178-0572
H Shakeel ⬤ https://orcid.org/0000-0002-0000-4621
M Litorja ⬤ https://orcid.org/0000-0003-1233-2179
J M Pomeroy ⬤ https://orcid.org/0000-0001-7848-7179

References

[1] Shons A, Dorman F and Najarian J 1972 *J. Biomed. Mater. Res.* **6** 565–70
[2] Thies J W, Kuhn P, Thrmann B, Dbel S and Dietzel A 2017 *Microelectron. Eng.* **179** 25–30
[3] Goyal A 2006 Ultrasensitive quartz crystal microbalance integrated with carbon nanotubes *PhD Thesis* Penn State University
[4] Kanazawa K K and Gordon J G 1985 *Anal. Chem.* **57** 1770–1
[5] Tsionsky V and Gileadi E 1994 *Langmuir* **10** 2830–5
[6] Davidson S, Berry J and Williams P 2018 *J. Phys.: Conf. Ser.* **1065** 042054
[7] Wei H and Pomeroy J 2016 *Metrologia* **53** 869–80
[8] Davidson S 2010 *Metrologia* **47** 487
[9] Bettin H and Schlamminger S 2016 *Metrologia* **53** A1–5
[10] Davidson S, Berry J, Abbott P, Marti K, Green R, Malengo A and Nielsen L 2016 *Metrologia* **53** A95
[11] Marti K, Fuchs P and Russi S 2015 *Metrologia* **52** 89–103
[12] Sauerbrey G 1959 *Z. Phys.* **155** 206–22
[13] Lu C S and Lewis O 1972 *J. Appl. Phys.* **43** 4385–90
[14] Mecea V M 1994 *Sensors Actuators* A **40** 1–27
[15] Mueller R M and White W 1968 *Rev. Sci. Instrum.* **39** 291–5
[16] Lu C S 1975 *J. Vac. Sci. Technol.* **12** 578–83
[17] Wajid A 1997 *Sensors Actuators* A **63** 41–6
[18] Shaw G A, Stirling J, Kramar J A, Moses A, Abbott P, Steiner R, Koffman A, Pratt J R and Kubarych Z J 2016 *Metrologia* **53** A86–94
[19] Brice J C 1985 *Rev. Mod. Phys.* **57** 105–46
[20] Janata J 1989 *Principles of Chemical Sensors* (New York: Plenum)
[21] Stock M, Davis R, de Mirandés E and Milton M J T 2019 *Metrologia* **56** 022001
[22] Newell D B 2014 *Phys. Today* **67** 35
[23] Picard A, Davis R, Gläser M and Fujii K 2008 *Metrologia* **45** 149
[24] Flux distribution and uniformity 2011 https://luxel.com/wp-content/uploads/2011/10/Flux-distribution-and-uniformity.pdf
[25] Fowler J and Litorja M 2003 *Metrologia* **40** S9–12